Evaluating microdefect structures by AFM-based deformation measurement

Vogel, Dietmar, Keller, Juergen, Gollhardt, Astrid, Michel, Bernd

Dietmar Vogel, Juergen Keller, Astrid Gollhardt, Bernd Michel, "Evaluating microdefect structures by AFM-based deformation measurement," Proc. SPIE 5045, Testing, Reliability, and Application of Micro- and Nano-Material Systems, (22 July 2003); doi: 10.1117/12.483826

SPIE.

Event: NDE for Health Monitoring and Diagnostics, 2003, San Diego, California, United States

Evaluating microdefect structures by AFM based deformation measurement

Dietmar Vogel[*a], Jürgen Keller[b], Astrid Gollhardt[a], Bernd Michel[a]
[a]Dept. Mech. Reliability and Micro Materials, Fraunhofer Institute for Reliability and Microintegration (IZM) Berlin
[b]Brandenburgische Technische Universität Cottbus, Chair of Polymeric Materials, Cottbus

ABSTRACT

The rapid development of a wide variety of new devises in microelectronics, sensor, MEMS, NEMS and nano technology will lead to new challenges for their mechanical characterization and reliability assessment. Measurement of deformations and stresses in microscopic and even nanoscopic regions becomes a key issue. The authors make use of load state images captured by Atomic Force Microscopes (AFM) in order to measure object deformations. Out-of-plane deformation is determined from usual topography scans by computing surface profile differences. NanoDAC, a recently established approach, allows to meet these goals with regard to in-plane deformation. The method bases on cross correlations analysis performed on AFM scans, which are captured from thermally and/or mechanically loaded samples. Finally, local 3D displacement fields and in-plane strain fields are measured. A description of the basic principles and the capability of the technique are given. Furthermore, the authors demonstrate the potential of the mentioned method by its application to microcrack evaluation and the study of sensor and MEMS structure degradation. The first application corresponds to the measurement of crack opening displacement in the very vicinity of crack tips. As a consequence, fracture mechanics parameters are derived and allow to assess the defect with regard to possible crack propagation and component failure. This approach is used to study the influence of nanoscale material structures on crack behavior. The second example illustrates how the impact of thermal loading to the constitution of sensor or MEMS submicron layers is investigated by deformation analysis. The devices had been heated actively under the AFM. Degradation processes due to a severe thermal material mismatch were observed and monitored.

Keywords: atomic force microscopy, displacement and strain, nanoDAC, DIC, crack evaluation, sensors, MEMS

1. INTRODUCTION

Recent advances in semiconductor and electronic, photonic and MEMS packaging technology have led to a strong need in stress/strain analysis on micro and nano scale. Different kind of thermo-mechanical reliability studies have to be accompanied by deformation measurements on real components and devices. Namely, smallest cracks, delaminations and material imperfections are a concern and may initiate defect propagation and cause failure of whole components. Because of the microscopic and even nanoscopic size of semiconductor and packaging structures traditional experimental methods for deformations measurement, like Moiré technique and laser speckle interferometry [1,2], run out of their capability. E.g., crack detection for crack lengths of only some micrometers is required. Simple optical microscopy, SEM and in some cases even AFM imaging will not allow to detect cracks, if they are closed or only slightly opened for different load states. Moreover, it has to be evaluated whether a crack of that size will propagate under external load or not. For that purpose fracture mechanics concepts have to be applied to existing cracks or delaminations under investigation. Parameters of fracture mechanics criteria more often must be determined directly from measured displacement or strain fields in the very vicinity of the crack tip.

On the other hand, measurement of deformation fields on loaded components and devices is a more general problem to be tackled for analysis of material degradation and failure behavior. Deformation measurement on micro- and

[*] dietmar.vogel@izm.fraunhofer.de; phone +49-30-46403200; fax +49-30-46403211; http://www.izm.fhg.de; Fraunhofer Institute for Reliability and Microintegration (IZM), Gustav-Meyer-Allee 25, D-13355 Berlin, Germany

Testing, Reliability, and Application of Micro- and Nano-Material Systems,
Norbert Meyendorf, George Y. Baaklini, Bernd Michel, Editors, Proceedings of SPIE
Vol. 5045 (2003) © 2003 SPIE · 0277-786X/03/$15.00

nanostructures allows to extract data about material response to environmental load, on development of imperfections and defects as well as on material properties themselves.

The described problems can be overcome, if displacement measurement tools are available with a measurement resolution in the subpixel region of high resolution images. With regard to Scanning Electron Microscopy (SEM) the authors had developed and established a displacement/strain measurement method, basing on cross correlation algorithms applied to SEM micrographs [3,4]. Objects under investigation are loaded thermally and/or mechanically inside the SEM. As a result an accuracy of approximately 0.1 pixel for lower and medium magnifications can be achieved, which means a final resolution of some nanometers in terms of displacement.

Until now, Scanning Force Microscopes (SFM) mainly are utilized as imaging tools for nanoscopic structures. Considering them as a measurement tool surface profile measurement as well as lateral pitch measurement, e.g. for semiconductor lines, have been established. The combination of AFM images and digital image correlation algorithms provides the ability to access very small scale deformations. The authors of the paper first have made use of SFM equipment for deformation field measurement [5,6]. Chasiotis / Knauss [7,8] and Soppa [9] used the same approach to measure strain fields from AFM micrographs. This paper reports results of the transfer of the correlation method to SFM imaging and its application to the analysis of material defects.

In section 2 the correlation method and its capability is discussed making emphasis to images captured by AFM. Section 3 demonstrates how to utilize AFM based deformation measurements for microcrack evaluation. The determination of stress intensity factors from crack opening displacement fields is shown. Potential application areas are discussed. Section 4 refers to the study of thermally induced material deterioration in thin films as applied in MEMS and sensor technology.

The advantage of SFM images are twofold: The higher lateral resolution of SFM in comparison to SEM provides better measurement resolution and SFM allow the scan of topography, i.e. real 3D displacement measurements can be carried out by a single method. In the following it is demonstrated, how the method can be applied to detect microcracks and measure load states images for crack evaluation by Linear Elastic Fracture Mechanics (LEFM). Potential applications on electronics components are discussed.

2. MEASUREMENT OF THERMALLY AND MECHANICALLY INDUCED DEFORMATIONS FROM AFM MICROGRAPHS

2.1 Measurement approaches

Object deformations can be extracted from AFM micrographs primarily as displacements fields. The latter are determined comparing micrographs of different object state, i.e. as a result incremental displacements are found. Commonly, the ***out-of-plane component*** of surface displacement vectors can be measured by the help of AFM topography scans. Assuming that images to be compared can be exactly matched with regard to their position, surface profile differences allow to calculate out-of-plane displacement fields realized in between the two states. A major challenge is the matching of images. During loading the cantilever has to be detached from the object in most of the cases. The AFM head with the cantilever cannot be repositioned with pixel accuracy during the subsequent approach, consequently numerical matching of the topography scans before and after load is necessary. Only afterwards surface profile subtraction can be carried out. Correlation algorithms described below for in-plane displacement measurements are a suitable tool to figure out the right image shift and rotation to be applied. As surface profile differences are obtained, possible object rotation around the two in-plane rotation axes has to be compensated. Finally, the possible measurement error due to time dependent scanning behavior of the AFM piezo has to be considered for small out of-plane displacement values. Any way, for larger deformations this effect can be neglected.

The measurement of the ***in-plane component*** of surface displacement vectors is more sophisticated and is described in more detail. Images picked up by Scanning Force Microscopes commonly exhibit local natural pattern, which can be utilized as unique markers for deformation measurements. Commonly these pattern maintain even during severe thermal or mechanical loading of objects. Consequently, incremental displacement fields can be determined from the

comparison of subsequent load state micrographs, applying cross correlation algorithms to a set of small image subwindows.

The correlation approach is illustrated by Fig. 1. Images of the object are obtained at a the reference load state 1 and at different second load state 2. Both images are compared with each other using a special cross correlation algorithm. In the image of load state 1 (reference) rectangular search structures (kernels) are defined around predefined grid nodes (Fig. 1, left). These grid nodes represent the coordinates of the center of the kernels. The kernels them-selves act as gray scale pattern from load state image 1 that have to be tracked, recognized and determined by their position in the load state image 2. In the calculation step the kernel window (n×n submatrix) is displaced inside the surrounding search window (search matrix) of the load state image 2 to find the best-match position (Fig. 1, right).

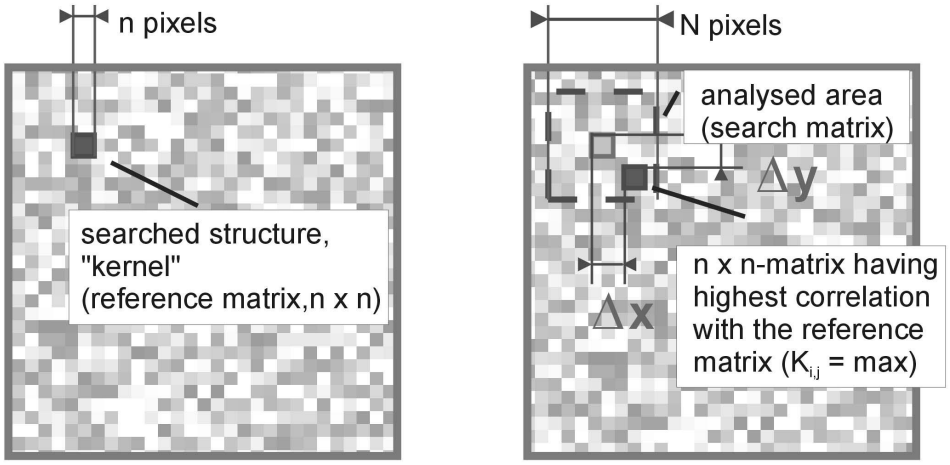

Fig. 1: Displacement evaluation by cross correlation algorithm; (left) reference image at load state 1; (right) image at load state 2 used for comparison

This position is determined by the maximum cross correlation coefficient, which can be obtained for all possible kernel displacements within the search matrix. The computed cross correlation coefficient *K* compares gray scale intensity pattern of load state images 1 and 2, which have the same size of the kernel. *K* is equal to:

$$K_{i',j'} = \frac{\sum_{i=i_0}^{i_0+n-1}\sum_{j=j_0}^{j_0+n-1}\left(I_1(i,j)-M_{I_1}\right)\left(I_2(i+i',j+j')-M_{I_2}\right)}{\sqrt{\sum_{i=i_0}^{i_0+n-1}\sum_{j=j_0}^{j_0+n-1}\left(I_1(i,j)-M_{I_1}\right)^2\sum_{i=i_0}^{i_0+n-1}\sum_{j=j_0}^{i_0+n-1}\left(I_2(i+i',j+j')-M_{I_2}\right)^2}} \quad (1)$$

$I_{1,2}$ and $M_{I_{1,2}}$ are the intensity gray values of the pixel (i,j) in the load state images 1 and 2 and the average gray value over the kernel size, respectively. i' and j' indicate the kernel displacement within the search matrix of load state image 2. Assuming quadrangle kernel and search matrix sizes $K_{i',j'}$ values have to be determined for all displacements given by $-(N-n)/2 \le i',j' \le (N-n)/2$.

The described search algorithm leads to a two-dimensional discrete field of correlation coefficients defined at integer pixel coordinates (i',j'). The discrete field maximum is interpreted as the location, where the reference matrix has to be shifted from the first to the second image to find the best matching pattern. Simple parabolic interpolation between neighboring cross correlation coefficients at integer pixel locations aims at the estimation of the correlation coefficient maximum at subpixel positions. This algorithm implemented quite often allows to get a subpixel accuracy of about 0.1 pixel. More advanced algorithms are more accurate, allow to reach subpixel accuracies up to 0.01…0.02 pixel for

common 8 bit depth digitizing, but demand sophisticated analysis and depend on the kind image sources and of data to be treated.

Fig. 2 illustrates the measurement principle by the help of two AFM micrographs. The micrographs correspond to a crack in an epoxy material, which is forced to open by an external load applied to the crack test specimen. The black arrows are the displacement vectors derived by correlation analysis. They have been drawn with a scaling factor of six compared to the size of the image. Pattern displacement can be recognized, following the small movement of pronounced pattern with regard to the fixed measurement grid. Obviously, the crack has been opened, i.e. the crack boundaries are moving away from each other.

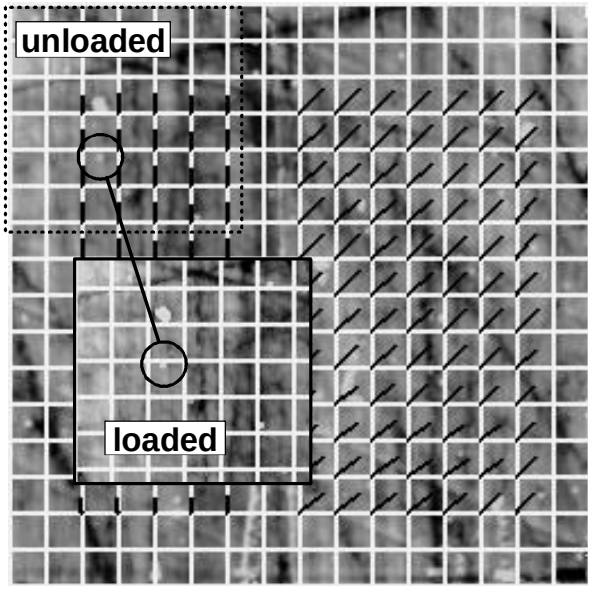

Fig. 2: Principle of displacement field measurement by the comparison of load state images, black arrows: displacement vectors in a regular grid of measurement point (6x enhanced vector size)

By computing derivatives of measured displacement fields it is possible to provide strain and rotation data. Besides the two in-plane displacement fields u_x and u_y the in-plane strains and the local in-plane rotation angle, respectively, are available:

$$\varepsilon_{xx} = \frac{\partial u_x}{\partial x}, \varepsilon_{yy} = \frac{\partial u_y}{\partial y}, \varepsilon_{xy} = \tfrac{1}{2}\left(\frac{\partial u_x}{\partial y} + \frac{\partial u_y}{\partial x} \right) \tag{2}$$

$$\rho_{xy} = \tfrac{1}{2}\left(\frac{\partial u_x}{\partial y} - \frac{\partial u_y}{\partial x} \right) \tag{3}$$

The correlation software allows two alternative ways to extract displacement and strain data from load state images. In the first case deformation data is determined for a grid of equidistant measurement points. In the second case deformation values are found for node points of a finite element mesh. The later approach implies that the mesh has been prepared for the object under investigation by the help of a FE preprocessor. The measurement at node points of a FE mesh aims at the direct comparison between results of finite element analysis and of results of corresponding measurements on real components. Fig. 3 shows a respective measurement example.

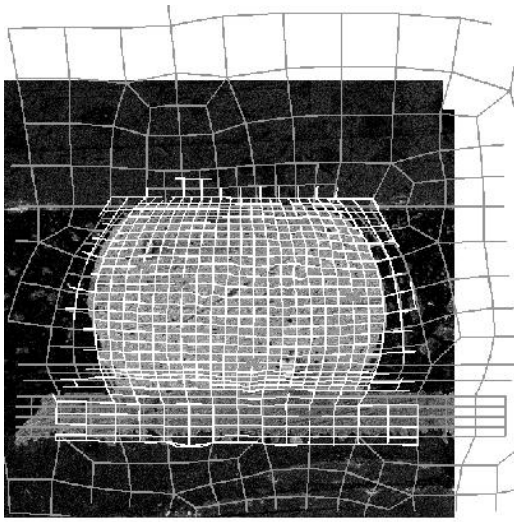

Fig. 3: Deformation measurement at a flip chip solder bump utilizing an ABAQUS finite element mesh, gray mesh: part of the complete undistorted FE mesh, white mesh: deformed FE mesh obtained from a measurement (displacement values 3 times enhanced), base micrographs: SEM images

2.2 Measurement accuracy

Measurement resolution is restricted by the level of scan digitizing as well as by the stability of the AFM scanning conditions. The resolution limit for displacement components u_x and u_y defined by the scan digitizing equals

$$\delta u_{x,y} = k_s \, L / M \tag{4}$$

where L indicates the absolute length of the AFM scan field. M is the number of pixels along this image edge and k_s is the achieved subpixel accuracy. As discussed above k_s reaches at least values of 0.1. I.e. for AFM scan sizes 1 µm × 1 µm and pixel arrays of 512 × 512 theoretically displacement measurements are feasible with an accuracy of 2 Å.

Unfortunately, stability and reproducibility of the AFM image scan are a concern and commonly reduce the finally obtained accuracy. Scanner drifts as well as to the extreme stability of the object needed over the image capture interval are an issue. The first problem implies an appropriate choice of AFM equipment with sufficient scanner stability, but also a high level of vibration and acoustic isolation of the AFM equipment. The second problem must be solved by a respective design of the loading stages and procedures, which allow to freeze load states for at least a minute.

As seen from Fig. 4 the microscope used by the authors exhibits a scanner stability, which does not reduce too significantly the measurement resolution as given by formula (4). For the stability check of Fig. 4 subsequent AFM images have been picked up, without loading the object. Therefore, evaluated displacements and strains represent only the measurement error. CMP treated silicon surfaces with ideal pattern have been chosen for this analysis. Obviously, higher line scan frequencies, i.e. smaller scan time, improve accuracy. Values along the cantilever line scan direction are more accurate, what should be expected from the same stability considerations. The standard deviation for displacements keeps near the level as known from microDAC measurements with SEM [4,6].

With a displacement measurement accuracy of 0.1 image pixel, strains can be determined approximately as accurate as $1 \cdot 10^{-3}$. Considering results of Fig. 4 somewhat higher measurement errors are found for strain values than expected from comparable data obtained earlier by optical or SEM based DIC measurements. It is assumed that improvements for strain measurement are possible, because no optimizations of data refinement procedures (smoothing, grid building algorithms) has been included.

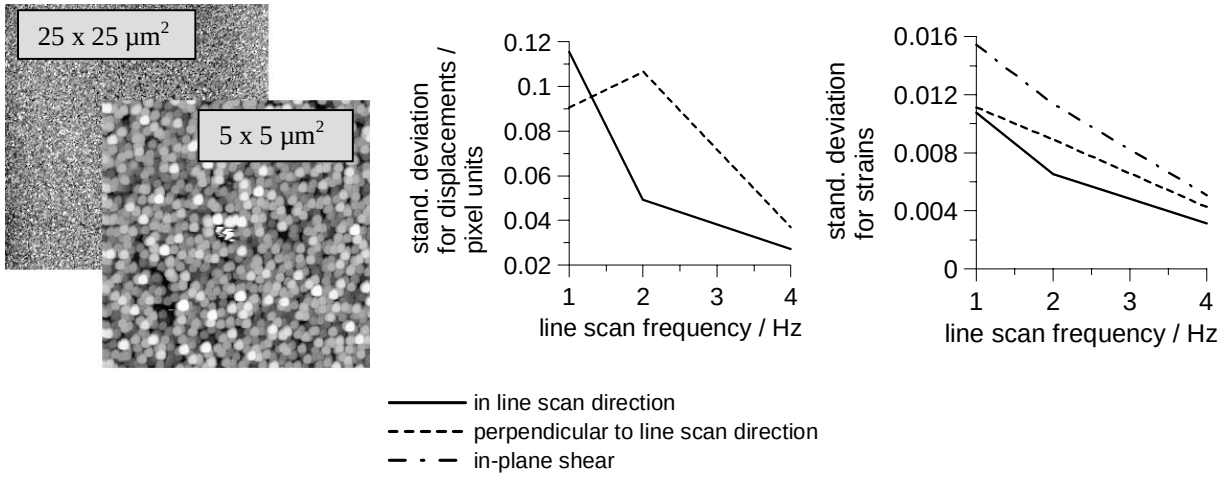

Fig. 4: Estimation of measurement errors for nanoDAC by the help of data standard deviation (over a whole image) determined for subsequently scanned, unaltered samples; non contact scan mode; left side: used Si specimens (sample roughness approx. 10 ... 20 nm); right side: error dependency over the applied line scan frequency

The lateral resolution of a single measurement point is a function of the local pattern size n (pixel units) used in cross correlation. Non overlapping of neighboring searched pattern must be provided for independent displacement values, i.e. the lateral resolution equals approximately

$$\delta l = L\, n / M \tag{5}$$

and is less than the pixel resolution of the image. Selecting M = 512 and typical values for n in between 10 and 40, lateral resolution is about 2 ... 8 % of the image edge length in absolute units.

3. MICROCRACK EVALUATION BY NANODAC MEASUREMENTS

Tiny defects or cracks present in micro electronics components can lead to severe crack propagation and complete failure if electronic devices are stressed. Because of intrinsic stress sources, like e.g. thermal material mismatches, also the change of environmental conditions (temperature, pressure, mechanical vibrations) can initiate fatal crack propagation. Experimental crack detection can be a crucial issue having in mind original crack sizes of about some micrometer. These cracks will open under subcritical load only some tens of nanometers or even less. Their detection is possible by nanoDAC displacement measurements. Fig. 5 shows as an estimation made by Finite Element Simulation for a typical case. The crack opening displacement of the microcrack in a chip passivation layer is as small as 20 nm for the critical load of the die bending. Fig. 6 shows an example of potential initial cracks, which are introduced in Si chip edges after wafer dicing.

Furthermore, the determination of real crack load in stressed components or devices can be a tough job, if ample data on material laws and properties required for Finite Element Analysis is uncertain. In this case it could be easier to determine fracture parameters form crack opening displacements, where material data is needed only for the adjacent to the crack materials. Taking into consideration the mentioned problems, first attempts have been made to measure parameters of simple fracture criteria like, e.g., stress intensity factors.

NanoDAC measurements of stress intensity factors are accomplished under the following assumptions, which have been made:

- linear Elastic Fracture Mechanics (LEFM) can be applied within the measurement area and loads,

- the specimen consists of homogeneous material,
- mode I and II mixing is allowed loading the component / specimen,
- the crack is parallel to the horizontal x-axis.

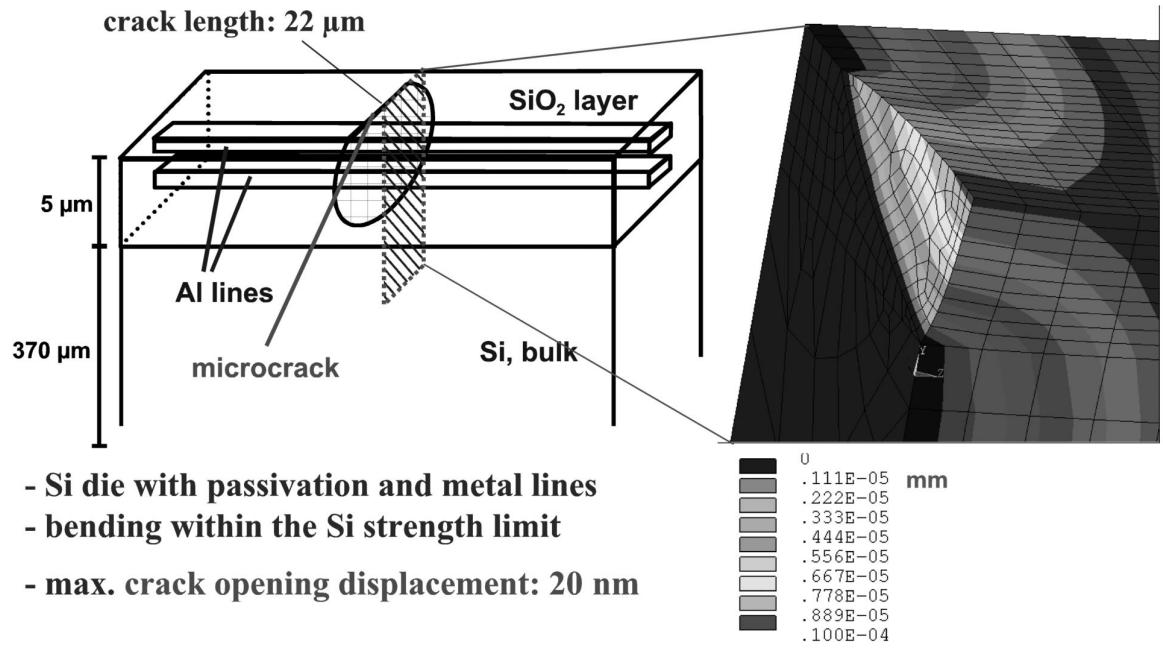

Fig. 5: Finite Element Simulation for a microcrack opening, crack location inside a chip passivation layer

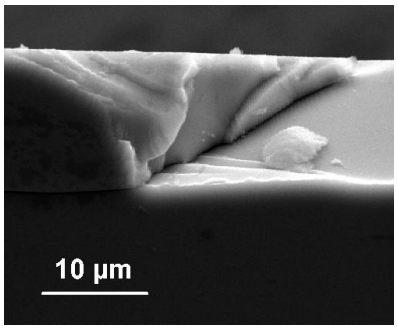

Fig. 6: Example of initial cracks occurring after wafer dicing at die edges

In order to determine the mode I stress intensity factor crack opening displacements u_y^u and u_y^l have been measured along both the upper and lower crack boundaries. If determined by LEFM they must equal to the values of Table 1.

Table 1: Crack opening displacement in LEFM for infinite bulk material and mode I crack opening

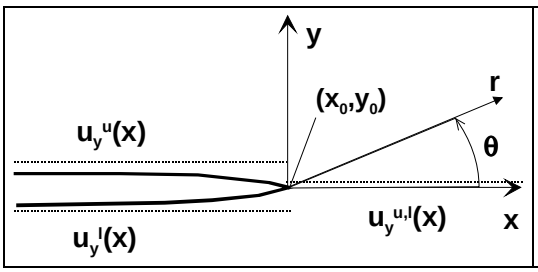	$u_y{}^u = \frac{K_I}{2\mu}\sqrt{\frac{x}{2\pi}}(k+1), \quad u_y{}^l = -\frac{K_I}{2\mu}\sqrt{\frac{x}{2\pi}}(k+1)$ for $x \le 0$ $u_y{}^u = u_y{}^l = 0$ for $x > 0$ (6)

In formula (6) E is the Young's modulus, ν the Poisson ratio, K_I the stress intensity factor and k a function of elastic material properties, somewhat different for plane stress or plane strain state [10]. Taking the square of the difference of upper and lower displacements we obtain a linear function of the x-coordinate or 0, in dependence, at which side of the crack tip we are:

$$\left(\frac{u_y{}^u - u_y{}^l}{2}\right)^2 = Cx \qquad x \le 0$$
$$= 0 \qquad x > 0 \tag{7}$$

Expression (6) does not change if specimen rotation due to load is included into the consideration. In this case equal rotational terms are subtracted from each other. For the formula above, the crack tip is set at position x = 0. The crack tip position on the real specimen can be found from the interception of a linear fit of the curve Cx with the x-coordinate axis. The incline C allows to estimate the stress intensity factor K_I, which is a measure of the crack tip load.

$$K_I = \frac{E}{1+\nu}\frac{1}{k+1}\sqrt{2\pi C} \tag{8}$$

Examples of used AFM images captured under mechanical load are given on Fig. 7.

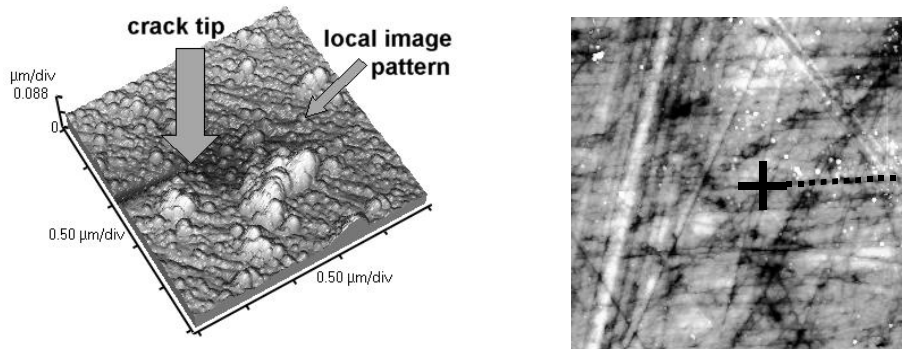

Fig. 7: Examples of typical AFM scans with crack used for nanoDAC analysis, right side: AFM image (size: 25 x 25 µm^2) with crack boundary line (·····) and crack tip position determined from the displacement fields (+)

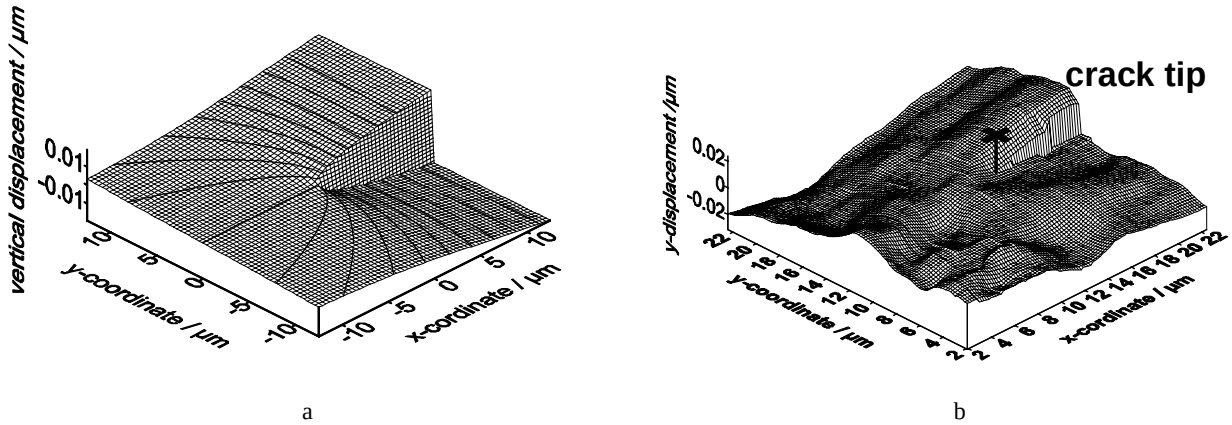

a b

Fig. 8: Displacement measurement from AFM images at the crack tip position, displacement fields u_y (component perpendicular to the crack boundaries), a – theoretic field from LEFM analytical solution for mode I crack opening, b – measured from AFM topography scans (25 µm x 25 µm image size)

Fig. 8 shows the ideal (theoretical) and the measured u_y displacement fields. Maximum crack opening in the measurement area is about 20 nm only (at the area edge). The stress intensity factor was estimated from the measured displacement field as $K_I = 0.0098$ MPa $m^{1/2}$. Comparing this value with the critical stress intensity factor $K_{IC} \approx 0.6$ MPa $m^{1/2}$ of the material, it should be mentioned that the applied crack load was about 1/60 of the critical value. The studied crack was characterized by a particular mode mixitiy. The stress intensity factor K_{II} for mode II crack opening has been also measured, but now making use of u_x values (displacements in crack direction) along the crack boundaries.

Fig. 9 shows an example of determined incremental stress intensity factors from crack opening displacements computed from SFM images making use of formula (7) and (8).

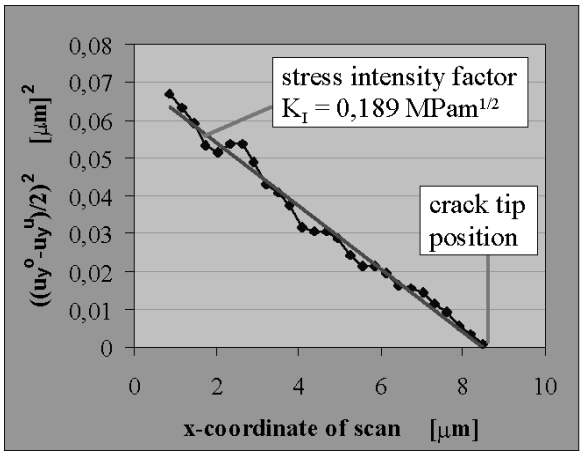

Fig. 9: Determination of stress intensity factors from crack tip displacement fields, obtained by AFM imaging

Fracture toughness values to a large extend depend on the material damage mechanisms in the highly stressed, submicron crack tip region. Therefore, nanoscale modified, nano-filled composite materials and nanoalloys are developed to improve thermo-mechanical material properties. NanoDAC deformation measurements are one tool giving access to phenomenological studies of material damage behavior of this kind of materials.

4. INVESTIGATION OF SENSOR AND MEMS STRUCTURES

Modern sensors and MEMS/NEMS devices consist of extremely fragile functional structures. Due to the desired device functionality, quite different materials in terms of material properties have to be combined with one another. Loading such structures thermally and/or mechanically means to implement severe material mismatch within submicron and nano-scale volumes. Therefore, functional or environmental loading causes local stresses and strains due to different material properties such as coefficient of thermal expansion (CTE), Young's modulus or time depended viscoelastic or creep properties. The smallest existing material imperfections or initial micro/nano-scale defects can grow under stress and strain and can finally lead to the failure of the device [10,11].

Thin layers used in sensor and MEMS technology undergo local stresses remote from elastic material behavior, where permanent device alterations are feared after each load cycle. Nowadays, responses of nanomaterials to applied external loads from temperature, vibrations, or chemical agents are not well understood. The same is true for actual failure mechanism and damage behavior. Moreover, quite often those structures escape from simple continuum mechanics and failure modeling and from respective numerical simulation, because material properties on micro and nano scale are not yet known or described in available databases. Furthermore, they may change over exploitation time. Due to this facts efforts have to be made to gain a better understanding of the material responses in submicron and nano regions [6,9].

The way to achieve this aim is the combination of displacement and strain measurements on the micro- and nanoscale with modeling techniques based on finite element analysis. Parameterized finite element models of MEMS are applied for faster prediction of life time and failure modes. The parameterization allows the variation of model geometries and materials in order to accelerate the MEMS design process [12].

In the following part an AFM based deformation analysis on a gas sensor membrane is represented. Sensor applications with local temperature regulation such as the gas sensor shown in Fig. 10 are usually thermally loaded with rapid and frequent change in temperature. This thermal cycling and the temperature gradients over the structure imply thermal stresses and may cause failure of the component [13] (see also Fig. 11). In the operation mode of the gas sensors thermal stresses are induced due to the activated PolySi microheater.

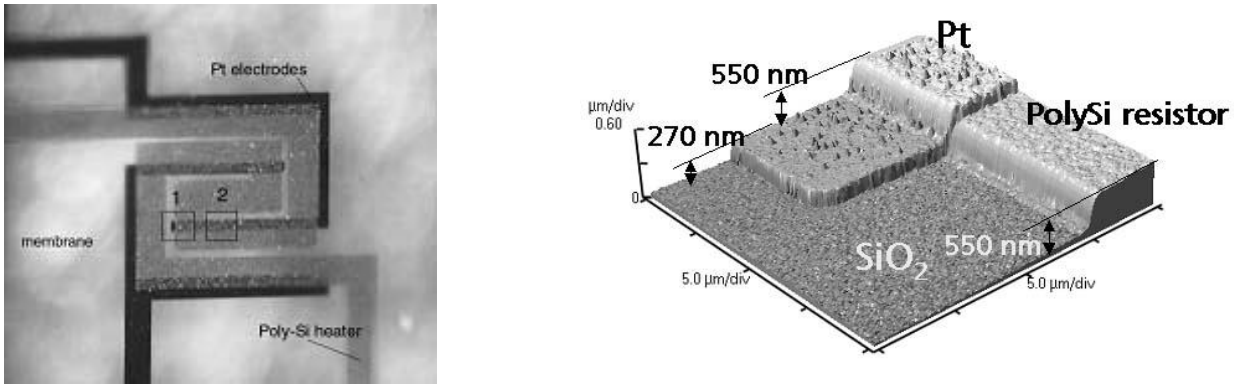

Fig. 10: left side: microscopic image of flow and gas sensor membrane, overall membrane thickness: approx. 2 µm, field of view: approx. 500 µm; right side: SFM topography scan of gas sensor depicting the Pt layer on top of the SiO_2 membrane and part of the Poly-Si heater embedded, Source: [14]

With in-situ SFM measurements on this microsystem the capability of the AFM based deformation measurement approach is demonstrated measuring material deformation resulting from mismatch of material properties. The height information of the SFM topography images before and after loading is analyzed for evaluation of movements or deformations in the z-direction. In-situ measurements of thermal deformations by AFM on the top of the sensor membrane have revealed a high value of remaining deformations even after a single heat cycle (25 to 100°C). Inelastic strains remain after cooling down to room temperature (Fig. 12). They can be the reason for more severe layer deterioration, if higher temperature pitch is applied.

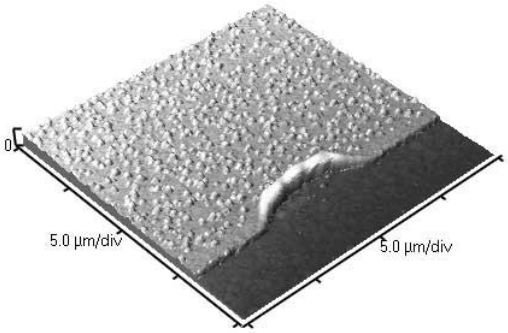

Fig. 11: SFM topography scan of membrane layers after tempering at 450 °C, Pt electrode destruction at edge and corners

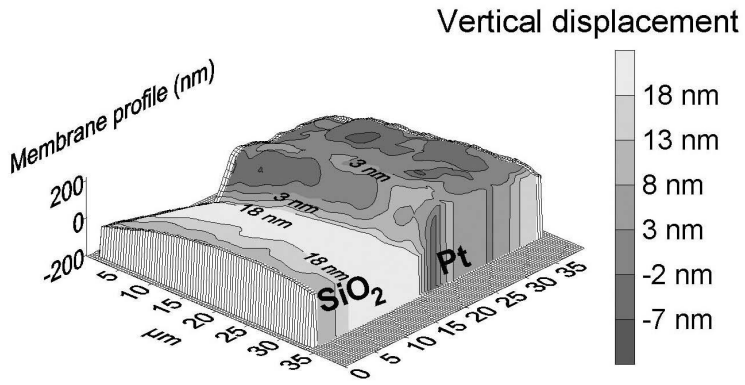

Fig. 12: Residual sensor deformation after heat cycle (SFM based deformation measurement), 3D plot shows part of the membrane layer profile, the coloring (gray scale) indicates the remaining vertical deformation after a heat cycle

5. CONCLUSIONS

It has been shown that Atomic Force Microscopy can be used to measure displacement and strain fields from micrographs captured for different object load states. Differences of height profiles allow to extract out-of-plane deformation. A digital image correlation (DIC) tool, nanoDAC, provides the in-plane components of deformation. Combining both methods, the complete displacement field, as well as in-plane strains, can be computed from AFM micrographs. The described approach is being used in connection with thermo-mechanical reliability analysis of components and devices from micro and nanotechnology. Namely, the evaluation of microcracks by fracture mechanics concepts and the investigation of heated sensor structures have been demonstrated as examples of the technique.

ACKNOWLEDGEMENTS

The authors wish to acknowledge the excellent collaboration with J. Puigcorbé of the Electronic Materials and Engineering (EME) research group, Department of Electronics, University of Barcelona and J.R. Morante of the Centre Nacional de Microelectrònica, Bellaterra, Barcelona.

The research was carried out in the Micro Materials Center Berlin (MMCB), which is partially funded by the German Federal Ministry of Research and Education (BMBF) in the MaTech Program under grant 03N6019.

REFERENCES

1. B. Han, Y. Gou, Thermal deformation analysis of various electronic packaging products by Moiré Interferometry, *J. of Electronic Packaging*, vol. 117, pp. 185-191, 1995.
2. K.J. Cote, M.S. Dadkhah, Whole Field Displacement Measurement Technique Using Speckle Interferometry, *Proc. of ECTC 2000*, Las Vegas, USA, May 2000.
3. D. Vogel, J. Simon, A. Schubert, B. Michel, High Resolution Deformation Measurement on CSP and Flip Chip, *Proc. of the Fourth VLSI Packaging Workshop of Japan*, pp. 84 – 86, Kyoto, Japan, Nov. 30 – Dec. 2 1998.
4. D. Vogel, et al.: Measurement of Thermally Induced Strains on Flip Chip and Chip Scale Packages, *Proc. of ITherm 2000*, pp. 232-239, Las Vegas, USA, May 2000.
5. D. Vogel, B. Michel: Microcrack Evaluation for Electronics Components by AFM nanoDAC Deformation Measurement, Proc. of IEEE-NANO 2001, Oct. 28-30, 2001, Maui, Hawaii, pp. 309-312.

6. D. Vogel, A. Gollhardt, B. Michel: Micro- and nanomaterials characterization by image correlation methods, Sensors and Actuators A 99 (2002) 165-171.
7. I. Chasiotis, W.G. Knauss: A new microtensile tester for the study of MEMS materials with the aid of Atomic Force microscopy, Experimental Mechanics, Vol. 42; No. 1, March 2002, pp. 51-57.
8. W.G. Knauss, I. Chasiotis ,Ying Huang: Mechanical measurements at the micron and nanometer scales, Mechanics of Materials, Vol. 35, 2003, pp. 217 –231.
9. E. Soppa, et. al: Experimental and numerical characterization of in-plane deformation in two-phase materials, Computational Material Science, Vol. 21, 2001, pp. 261-275.
10. D. Vogel, J. Auersperg, B. Michel: Characterization of Electronic Packaging Materials and Components by Image Correlation Methods. Advanced Photonic Sensors and Applications II, Nov. 27-30, 2001, Singapore, Proc. of SPIE, Vol. 4596, pp. 237-247.
11. C.B. O'Neal, et al.: A Study of the Effects of Packaging Induced Stress on the Reliability of the Sandia MEMS Microengine. Proc. of IPACK2001: The Pacific Rim/ASME International Electronic Packaging Technical Conference and Exhibition, July 8-13, 2001, Hawaii, USA.
12. J. Auersperg, R. Döring, B. Michel: Gains and Challenges of Parameterized Finite Element Modeling of Microelectronics Packages, Micromaterials and Nanomaterials, No. 1, 2002, ed. by B. Michel, Fraun-hofer IZM, Berlin, pp. 26-29.
13. J. Puigcorbé, A. Vilà, J. Cerdà, A. Cirera, I. Gràcia, C. Cané and J. R. Morante: Thermo-mechanical Analysis of Micro-drop Coated Gas Sensors, Sensors and Actuators A, Vol. 97, 2002, pp. 379-385.
14. J. Puigcorbé, et al.: AFM Analysisof High Temperature Degradation in MEMS Elements, to be published in Proc. of MME'02, The 13th Micromechanics Europe Work-shop, October 6-8, 2002, Sinaia, Romania.